FAST ORBIT FEEDBACK CONTROL IN MODE SPACE*

S. Gayadeen [†], S.R. Duncan, University of Oxford, Oxford, OX1 3PJ, UK
M.T. Heron, Diamond Light Source, Didcot, OX11 0DE, UK

Abstract

This paper describes the design and implementation of fast orbit feedback control in mode space. Using a Singular Value Decomposition (SVD) of the response matrix, each singular value can be associated with a spatial mode and enhanced feedback performance can be achieved by applying different controller dynamics to each spatial mode. By considering the disturbance spectrum across both dynamic and spatial frequencies, controller dynamics for each mode can be selected. Most orbit feedback systems apply only different gains to each mode however; mode space control gives greater flexibility in control design and can lead to enhanced disturbance suppression. Mode space control was implemented on the Booster synchrotron at Diamond Light Source, operated in stored beam mode. Implementation and performance of the mode space controller are presented.

INTRODUCTION

Most fast orbit feedback (FOFB) controller designs decouple control into space and time domains. Spatial control involves the inverse of the steady state response matrix which is normally ill-conditioned. To resolve the ill-conditioning, Singular Value Decomposition (SVD) of the response matrix is performed and the less significant singular values are removed or filtered. For dynamic control, the common approach for synchrotron FOFB is to use proportional-integral (PI) control [1–4]. In this paper, an Internal Model Control (IMC) structure is used to design the controller dynamics [5]. The good stability characteristics of IMC based designed controllers are well-known and for this type of stabilising control problem, this is an important factor. The use of IMC is also motivated by explicit design trade-offs and flexibility for tuning.

To reduce computation for FOFB systems, the same controller is usually applied to each mode but the controller bandwidth is adjusted by applying a different gain, resulting from the pseudo-inverse of the response matrix. However applying different dynamics to individual modes (referred to mode space control) gives greater flexibility in control design and can lead to enhanced disturbance suppression. In this paper, a two-dimensional loop shaping technique is adapted from [6] where the dynamics for each mode are selected based on the dynamic frequency content of the disturbance at that mode.

In order to apply different dynamics to individual modes, two matrix multiplications are required; one to convert the error into mode space before applying the controller

dynamics and then another to convert from mode space to input space. This is usually too computationally heavy for most Storage Ring FOFB control systems which have >100 actuators and update rates greater than a few kHz. Smaller and slower systems though are able to handle the computation of the two matrix multiplications, such as the SPEAR3 FOFB controller, which updates at 4 kHz and has just 56 BPMs and 14 correctors and therefore can apply different dynamics to individual modes [1]. Likewise, the Booster synchrotron at Diamond, which has similar hardware as the Storage Ring, has 22 sensors and 22 actuators rather than the 172 sensors and 172 actuators on the Storage Ring. When operated in stored beam mode, the Booster acts as a test bed for FOFB development and mode space control has been implemented. The results of the mode space controller using the loop shaping technique is presented in this paper.

CONTROLLER DESIGN

In practice the control system is implemented in "sample and hold" mode where the sensor takes M beam position measurements $\mathbf{y}[k]$ at times $\{t = kT_s : k \in \mathbb{Z}^+\}$, with T_s being the sample interval so that $\mathbf{y}[k] = \mathbf{y}(kT_s)$ and the N actuator inputs, $\mathbf{u}[k]$ are held constant over the time interval $t \in [kT_s, (k+1)T_s]$ [5]. The open loop response in discrete time can be expressed as,

$$\mathbf{y}[k] = g(z^{-1})\mathbf{R}\mathbf{u}[k] + \mathbf{h}[k] \qquad (1)$$

where the response matrix $\mathbf{R} \in \mathbb{R}^{M \times N}$ is the steady state response of the actuators, $\mathbf{h}[k]$ is the disturbance and $g(z^{-1})$ is the scalar dynamics, assumed to be the same for all actuators, given by

$$g(z^{-1}) = z^{-d}\frac{b_0 + b_1 z^{-1}}{1 - a_1 z^{-1}} \qquad (2)$$

where d is the smallest integer satisfying $dT_s > \tau_d$ and

$$\begin{aligned} a_1 &= e^{-aT_s} \\ b_0 &= 1 - e^{a(T_s - \tau')} \\ b_1 &= e^{a(T_s - \tau')} - e^{-aT_s} \end{aligned} \qquad (3)$$

with $\tau' = \tau_d - (d-1)T_s$ such that τ_d is the delay in the system and a is the bandwidth of the actuator response (in rad.s^{-1}) [5]. For $M \leq N$, the singular value decomposition of $\mathbf{R}$ takes the form,

$$\mathbf{R} = \mathbf{\Phi}\left[\mathbf{\Sigma}\ \mathbf{0}\right]\mathbf{\Psi}^{\mathrm{T}} \qquad (4)$$

where $\mathbf{\Phi} \in \mathbb{R}^{M \times M}$ and $\mathbf{\Psi} \in \mathbb{R}^{N \times N}$ are respectively the left and right singular vectors and $\mathbf{\Sigma} \in \mathbb{R}^{M \times M}$ is a
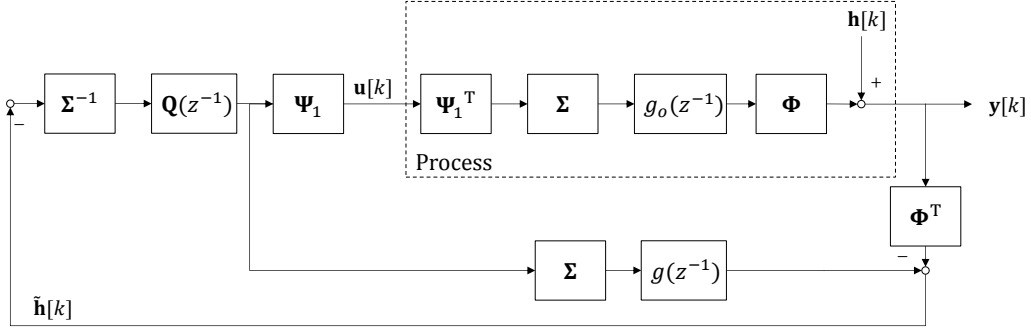
Figure 1: IMC controller structure.

diagonal matrix containing the singular values, $\sigma_1 \geq \sigma_2 \geq \cdots \geq \sigma_M$. By partitioning $\boldsymbol{\Psi}^{\mathrm{T}}$ as $\begin{bmatrix} \boldsymbol{\Psi}_1 & \boldsymbol{\Psi}_2^{\mathrm{T}} \end{bmatrix}^{\mathrm{T}}$ where $\boldsymbol{\Psi}_1^{\mathrm{T}} \in \mathbb{R}^{M \times N}$ and $\boldsymbol{\Psi}_2^{\mathrm{T}} \in \mathbb{R}^{(N-M) \times N}$, so that

$$\mathbf{R} = \boldsymbol{\Phi} \boldsymbol{\Sigma} \boldsymbol{\Psi}_1^{\mathrm{T}} \qquad (5)$$

then (1) can be written as

$$\boldsymbol{\Phi}^{\mathrm{T}} \mathbf{y}[k] = g(z^{-1}) \boldsymbol{\Sigma} \boldsymbol{\Psi}_1^{\mathrm{T}} \mathbf{u}[k] + \boldsymbol{\Phi}^{\mathrm{T}} \mathbf{h}[k]. \qquad (6)$$

Defining $\bar{\mathbf{y}}[k] = \boldsymbol{\Phi}^{\mathrm{T}} \mathbf{y}[k]$, $\bar{\mathbf{u}}[k] = \boldsymbol{\Psi}_1^{\mathrm{T}} \mathbf{u}[k]$ and $\bar{\mathbf{h}}[k] = \boldsymbol{\Phi}^{\mathrm{T}} \mathbf{h}[k]$ projects the response into "modal space", so that

$$\bar{y}_m[k] = g(z^{-1}) \sigma_m \bar{u}_m[k] + \bar{h}_m[k] \qquad (7)$$

where $\bar{y}_m[k]$, $\bar{u}_m[k]$ and $\bar{h}_m[k]$ are the mth elements of $\bar{\mathbf{y}}[k]$, $\bar{\mathbf{u}}[k]$ and $\bar{\mathbf{h}}[k]$.

The structure of an Internal Model Control (IMC) system is shown in Fig. 1. IMC is an advantageous structure because the error signal $\tilde{\mathbf{h}}[k]$, given by

$$\tilde{\mathbf{h}}[k] = \bar{\mathbf{h}}[k] + \boldsymbol{\Sigma} \left[g_0(z^{-1}) - g(z^{-1}) \right] \bar{\mathbf{u}}[k] \qquad (8)$$

acts on both the disturbance, $\bar{\mathbf{h}}[k]$ and the effect of any mismatch between the real process, $g_0(z^{-1})$ and the plant model $g(z^{-1})$. Additionally, because the parallel path containing the plant model is included, this structure inherently handles systems with delays. The assumption that all the actuators have the same dynamics allows the individual modes to be controlled independently, so that

$$\mathbf{Q}(z^{-1}) = \mathrm{diag}\{q_m(z^{-1})\} \qquad (9)$$

where $q_m(z^{-1})$, the pseudo plant inverse dynamics are described by the scalar transfer function,

$$q_m(z^{-1}) = \frac{(1 - \lambda_m)}{1 - \lambda_m z^{-1}} \frac{1 - a_1 z^{-1}}{(b_0 + b_1)}. \qquad (10)$$

where $\lambda_m = e^{-\zeta_m T_s}$ and ζ_m is a tuning parameter which is different for each mode. The IMC structure in Fig. 1 can be rearranged as in Fig. 2 so that the controller becomes

$$\mathbf{C}(z^{-1}) = \boldsymbol{\Psi}_1 \mathrm{diag} \left\{ \frac{1}{\sigma_m} c_m(z^{-1}) \right\} \boldsymbol{\Phi}^{\mathrm{T}} \qquad (11)$$

where the controller dynamics for each mode are

$$c_m(z^{-1}) = \frac{q_m(z^{-1})}{1 - g(z^{-1}) q_m(z^{-1})}. \qquad (12)$$

Substituting for $g(z^{-1})$ from (2) and $q_m(z^{-1})$ from (10) gives

$$c_m(z^{-1}) = \frac{(1 - \lambda_m)}{(b_0 + b_1)} \frac{1 - a_1 z^{-1}}{1 - \lambda_m z^{-1} - z^{-d}(1 - \lambda_m)\beta(z^{-1})} \qquad (13)$$

where

$$\beta(z^{-1}) = \beta_0 + \beta_1 z^{-1} = \frac{b_0 + b_1 z^{-1}}{b_0 + b_1}. \qquad (14)$$

Because $\beta_0 + \beta_1 = 1$ and the presence of the $(1 - z^{-1})$ term in the expansion of (13), the controller takes the form of a Dahlin controller [5, 7] and as a result, includes integral action. The controller is designed by choosing a different tuning parameter ζ_m (and hence λ_m) for each mode, and as a result, each mode has its own dynamics [5].

Fig. 3 shows a colour map of the average power (in dB) at each frequency within each of the modes for the Booster and it can be seen that the bulk of the power is concentrated in the lower order modes (i.e. for $m < 10$) and at frequencies <100 Hz, with a major peak at 50Hz. Large variations are also present at low frequencies (< 1Hz) and in practice, these are caused by a slow drift over time periods of the order of 10s. The aim of the control system is to reduce the effect of the disturbances on the beam particularly for the low order modes at frequencies < 100 Hz, while at the same time attenuating low frequency disturbance (< 1Hz) in all modes. The control system also needs to be robust to uncertainties in the model which have the biggest effect when controlling the higher order modes. The control design needs to balance these conflicting requirements and reduces to the choice of suitable values for ζ_m which will provide sufficient bandwidth to attenuate the disturbances and controller gains that will focus the control effort on the lower order modes. However the controller also needs to provide attenuation at low frequencies for all modes, in order to respond to the slow drift in the electron beam.
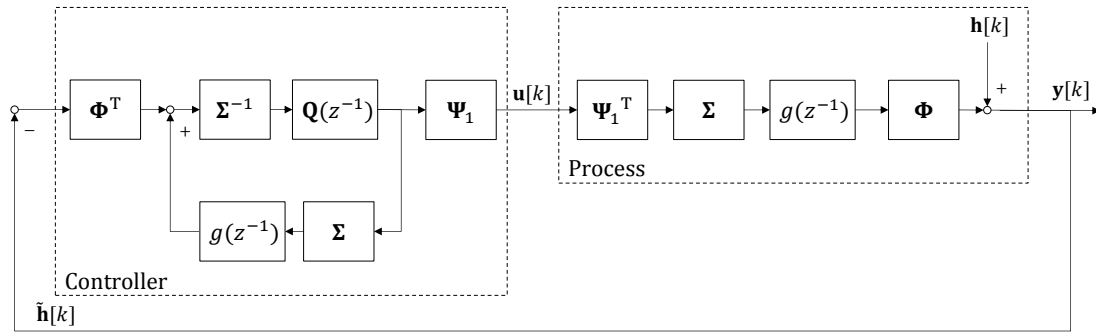
Figure 2: Alternative IMC controller structure that is suitable for implementation.

One way of choosing the dynamics of the controller is given by

$$\mathbf{C}(z^{-1}) = \mathbf{\Psi}_1 \mathbf{L} \mathbf{\Sigma}^{-1} c(z^{-1}) \mathbf{\Phi}^{\mathrm{T}} \qquad (15)$$

where $\mathbf{L} = \mathrm{diag}\{l_m\}$ is a gain matrix chosen to ensure that the optimal control action is applied to the low order modes, but the control action is "switched off" for the high order modes where the effect of modelling uncertainties is greatest and the control actions tend to be large. A possible choice for the values of l_m is derived from the Tikhonov regularisation [8] where small singular values are filtered out, so that

$$l_m = \frac{\sigma_m^2}{\sigma_m^2 + \mu} \qquad (16)$$

where μ is chosen such that $l_m \approx 1$ when $\sigma_m^2 \gg \mu$ and $l_m \to 0$ when $\sigma_m^2 \ll \mu$. In addition, a different ζ_m is selected for each mode. It is common to select ζ_m such that the time constant of the closed loop response is equivalent to the delay, so that

$$\zeta_m = 1/\tau_d \qquad (17)$$

which gives $\lambda_m = e^{-T/\tau_d}$ [9]. The sensitivity function is the transfer function from the disturbance $\bar{\mathbf{h}}[k]$ to the output $\bar{\mathbf{y}}[k]$, given by

$$s_m(z^{-1}) = \frac{1 - \lambda_m z^{-1} - z^{-d}\beta(z^{-1})}{1 - \lambda_m z^{-1} - z^{-d}(1 - l_m)(1 - \lambda_m)\beta(z^{-1})} \qquad (18)$$

where l_m and λ_m are chosen to shape the sensitivity function for each mode to match the disturbance content of that mode.

CONTROLLER IMPLEMENTATION

Booster Controller Realisation

Electron BPMs are used to provide information about the electron beam position at a sampling rate of 10 kHz. The Booster has 22 cells arranged as 4 sectors each of which has a computation node which receives all sensor positions but only calculates the local corrector magnet error. To achieve the required 10 kHz update rate, a custom communication controller implemented in VHDL is used to transmit the horizontal and vertical data from the 22 BPMs to each of the 4 computation nodes. Each computation node receives data from all BPMs and uses a dedicated VME processor card to calculate the vector product of the BPM values and $\mathbf{\Phi}^{\mathrm{T}}$. The controller dynamics are then implemented as an eighth order IIR filter on these values. The result then is multiplied by $\mathbf{\Psi}_1$ which corresponds to the new values for the local corrector magnets for that sector [10, 11].

Booster Controller Dynamics and Performance

For the Booster, (17) corresponds to a closed loop bandwidth of $\zeta_m = 1.43 \times 10^3$ rad.s^{-1} or 227 Hz. However for low order modes, this choice of ζ_m is too conservative, as the bulk of the disturbance is concentrated at these modes. So instead, ζ_m for each mode is chosen as below,

$$\begin{aligned} \zeta_{m=1,\dots,15} &= 1/1.2\tau_d & = 189 \text{ Hz} \\ \zeta_{m=16,\dots,22} &= 1/\tau_d & = 227 \text{ Hz}. \end{aligned} \qquad (19)$$

On Fig. 3 the 0dB sensitivity function contour is shown with ζ_m in (19) for two different values of μ. The sensitivity contour marks the region where the controller suppresses the disturbance. By decreasing μ, the controller bandwidth is increased and control is extended to higher order modes which results in further reduction of beam variation. However, this will result in a controller that is more sensitive to modelling errors and may lead to instability [12]. For the Booster controller, with $\mu = 1$, the sensitivity function for the first mode is shown in Fig. 4. It can be seen that the controller suppresses disturbances up to 100Hz and with a maximum suppression of 40dB at 1Hz. In Fig. 5, the vertical integrated beam motion for the corrected beam using different dynamics on each mode is compared to using only different gains on each mode selected by (16). It can be seen that there is significant improvement of the beam motion especially at high frequencies.

CONCLUSIONS

In this paper the design and implementation of a mode space FOFB controller on the Booster synchrotron
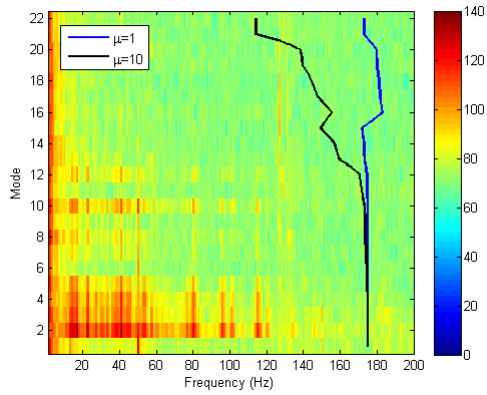
Figure 3: Colormap of Booster average power (dB) for each mode against frequency (Hz) showing 0dB sensitivity contours for $\mu = 1$ (blue) and $\mu = 10$ (black).
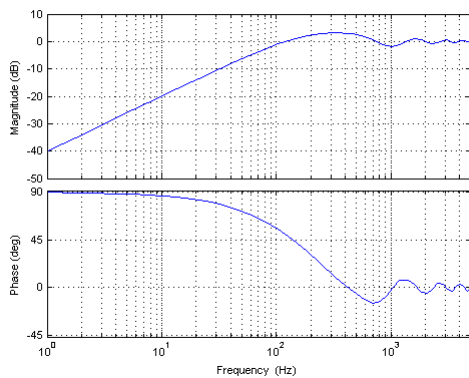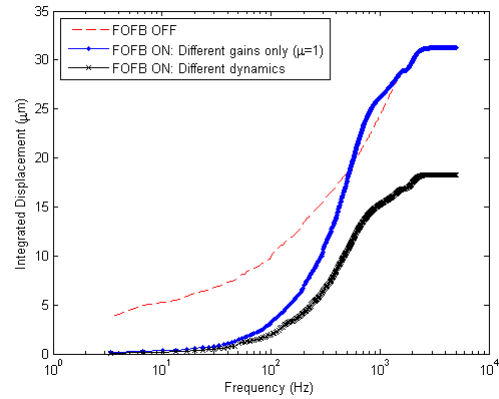

Figure 5: Booster vertical integrated beam motion for uncontrolled ('- -' red), and for the controlled beam when the controller for individual modes has different gains ('.-' blue) and when the controller for individual modes has different dynamics ('x-' black).

Figure 4: Booster frequency response of sensitivity function for the first vertical mode.

at Diamond is described. The aim of the controller is to reduce the effect of disturbances on the electron beam particularly at low order modes and attenuate low frequency disturbances. By applying different dynamics on each mode tailored to match the frequency content of the disturbance in both spatial and dynamic domains, improved disturbance rejection is achieved over applying different gains only on individual modes.

REFERENCES

[1] A. Terebilo and T. Straumann. Fast global orbit feeback system in SPEAR3. In *10th European Particle Accelerator Conference*, Edinburgh, Scotland, 2006.

[2] D. Beltran and M. Muñoz. Initial design of a global fast orbit feedback system for the ALBA synchrotron. In *ICALEPCS*, Knoxville, Tennessee, 2007.

[3] J.M. Koch, F. Epaud, E. Plouviez, and K. Scheidt. Fast orbit correction for the ESRF storage ring. In *ICALEPCS 2011*, Grenoble, France, October 2011.

[4] Y. Tian and L. Hua. NSLS-II fast orbit feeback with individual eigenmode compensation. In *ICALEPCS 2011*, Grenoble, France, October 2011.

[5] S.R. Duncan. The design of a fast orbit beam stabilisation system for the diamond synchrotron. Technical Report 2296/07, University of Oxford, 2007.

[6] G.E. Stewart. Two-dimensional loop shaping. *Automatica*, 39:779–792, 2003.

[7] D. Seborg, T. Edgar, D. Mellichamp, and F. Doyle III. *Process Dynamics and Control*. John Wiley and Sons, 2011.

[8] Gene H. Golub and Charles F. Van Loan. Tikhonov regularization and total least squares. *SIAM J. Matrix Anal. Appl.*, 21(1):185–194, 1999.

[9] M. Morari and E. Zafiriou. *Robust Process Control*. Prentice-Hall, Englewood Cliffs, NJ, 1989.

[10] J. Rowland, M.G. Abbott, J.A. Dobbing, M.T. Heron, I. Martin, G. Rehm, and I. Uzun. Status of the Diamond fast orbit feedback system. In *ICALEPCS*, Knoxville, Tennessee, 2007.

[11] S. Gayadeen, S. R. Duncan, C. Christou, M.T. Heron, and J.Rowland. Diamond Light Source Booster fast orbit feedback system. In *ICALEPCS 2011*, Grenoble, France, October 2011.

[12] S. Gayadeen and S. Duncan. Uncertainty modeling and robust stability analysis of a synchrotron electron beam stabilisation control system. In *2012 IEEE 51st Annual Conference on Decision and Control (CDC)*, pages 931–936, Maui, HI, 2012.